Analyst

# Enzyme-Linked Immunosorbent Assay Utilizing Thin-Layered Microfluidics



| | |
|---|---|
| Journal: | *Analyst* |
| Manuscript ID | AN-ART-08-2019-001491.R1 |
| Article Type: | Paper |
| Date Submitted by the Author: | 07-Sep-2019 |
| Complete List of Authors: | Nakao, Tatsuro; The University of Tokyo, School of Engineering<br>Mawatari, Kazuma; The University of Tokyo,<br>Kazoe, Yutaka; The University of Tokyo<br>Mori, Emi; The University of Tokyo, School of Engineering<br>Shimizu, Hisashi; The University of Tokyo, International Research Center for Neurointelligence<br>Kitamori, Takehiko; The University of Tokyo, |
| | |

# Enzyme-Linked Immunosorbent Assay Utilizing Thin-Layered Microfluidics

Tatsuro Nakao[1], Kazuma Mawatari[1,2], Yutaka Kazoe[2], Emi Mori[2], Hisashi Shimizu[2] and Takehiko Kitamori[1,2*]

1 Department of Bioengineering, School of Engineering, The University of Tokyo, 7-3-1 Hongo, Bunkyo, Tokyo 113-8656, Japan

2 Department of Applied Chemistry, School of Engineering, The University of Tokyo, 7-3-1 Hongo, Bunkyo, Tokyo 113-8656, Japan

*Correspondence

Dr. Takehiko Kitamori, Department of Applied Chemistry, The University of Tokyo

6A01 Engineering Building No.3, Hongo 7-3-1, Bunkyo, Tokyo 113-0001, Japan

Email: kitamori@icl.t.u-tokyo.ac.jp

Phone: +81-3-5841-7231

Fax: +81-3-5841-6039

**Abstract**

A rapid and sensitive enzyme-linked immunosorbent assay (ELISA) is required for on-site clinical diagnosis. Previously, a microfluidic ELISA in which antibody-immobilized beads are packed in a microchannel for a high surface-to-volume (S/V) ratio was developed, but utilizing beads lead to complicated fluidic operations. Recently, we have reported nanofluidic ELISA that utilizes antibody-immobilized glass nanochannels ($10^2$-$10^3$ nm) to achieve high S/V ratio without beads, enabling even single-molecule detection, but it is not applicable to clinical diagnosis owing to fL sample volume much smaller than nL-μL sample volume in clinical diagnosis. Here, we propose an antibody-immobilized, thin-layered microfluidic channel as a novel platform. Based on the method of nanofluidic ELISA, the channel width was expanded from $10^3$ nm to $10^0$ mm to expand the volume of the reaction field to $10^2$ nL, while the channel depth ($10^3$ nm) was maintained to retain the high S/V ratio. A device design which incorporate a taper-shaped interface between the thin-layered channel and microchannel for sample injection was proposed, and the uniform introduction of sample into the high-aspect-ratio (width/depth ~ 200) channel was experimentally confirmed. For the proof of concept, a thin-layered ELISA device with the same S/V ratio as the bead-based ELISA format was designed and fabricated. By measuring a standard C-reactive protein solution, the working principle was verified. The limit of detection was 34 ng/mL, which was comparable to bead-based ELISA. We believe the thin-layered ELISA can contribute to medicine and biology as a novel platform for sensitive and rapid ELISA.

(247 words)

## 1. Introduction

Sensitive and rapid analysis of proteins is required for on-site clinical diagnosis. For example, an increasing demand exists for sensitive detection (~ng/mL) of biomarker proteins (PSA, Her2, etc.) for early diagnosis of severe diseases (e.g., cancers).[1,2] Enzyme-linked immunosorbent assay (ELISA) is a widely used method of quantifying proteins due to its high reproducibility and selectivity.[3] However, conventional 96-well plate ELISA requires multiple washing steps and long incubation times for each step of the reaction, making the assay laborious and time-consuming (typically, half-a-day for the total assay time). Therefore, a sensitive and rapid ELISA format is required.

To meet this demand, miniaturization of ELISA using microfluidic devices has been investigated.[4–10] Microfluidics has many advantages over conventional macroscale chemistry, including faster reaction due to limited diffusion length, ease of automation, reduced amount of precious and expensive reagents, etc.[11] In 2000, we reported the first format for microfluidic ELISA that utilizes packed beads in a microfluidic channel.[4] Highly sensitive (~ng/mL) and rapid (12 min) quantification has been achieved by increasing the surface-to-volume (S/V) ratio $10^2$-fold (compared to a 96-well plate) with packing of antibody-immobilized beads in the microfluidic channel.[5] This format was applied for detection of Immunoglobulin A,[4] Immunoglobulin E,[5] Interferon γ,[6] carcinoembryonic antigens[7] and brain natriuretic peptide[8] and has already been commercialized. Also, this beads-based format is reported using magnetic beads,[9] or in a centrifugal microfluidic layout.[10] However, some operational issues exist including a requirement for a complicated fluidic system for filling in/out of beads and difficulties with removing bubbles in between the densely packed beads.

Those issues can be solved by creating a high S/V reaction field without packing beads, and some bead-free formats for microfluidic ELISA have been proposed.[12–18] In one case, a microfluidic channel with an antibody-immobilized surface is used as a reaction field.[12–16] Although this method enables operation without a complicated fluidic system and easy removal of bubbles, the S/V ratio is still lower ($10^1$-fold of a 96-well plate) than the bead-based format ($10^2$-fold of a 96-well plate). Although some

methods to increase the sensitivity in this format are (e.g. enhancing the enzymatic amplification by modifying the detection antibodies)[16] are proposed, to realize high detection sensitivity in such low-S/V-ratio reaction field, long incubation time (typically >30 min.) is required for each step, leading to a long assay time (~h) Another method that uses 3-dimensional hydrogel co-polymerized with antibody-immobilized solid supports was proposed.[17,18] Although this method achieves a high S/V inside the hydrogel (>$10^2$-fold of a 96-well plate) and is free from operational difficulties, the increase in the S/V ratio is limited to the hydrogel, and could lead to potential escape of the analyte protein.

On the other hand, our group has expanded research on microfluidics to the even smaller space of $10^1$-$10^3$ nm, which we designate as an extended nanospace. We have established a fabrication method on a glass substrate of well-regulated nanochannels,[19] a fluidic control method by external pressure,[20] and a surface control method by bottom-up modification.[21] Based on those basic technologies, we have recently developed a nanofluidic ELISA.[22] Utilizing the high S/V reaction field of the nanochannel ($10^3$-fold of a 96-well plate), the nanofluidic ELISA can capture target antigens quickly (<1 min) and efficiently (almost 100%) and enables even single-molecule detection. Although this is a powerful tool for analyzing ultra-small amounts of proteins (e.g., proteins from single cells), this device is not applicable to clinical diagnosis due to the ultra-small size of the nanochannels. The reaction field of nanofluidic ELISA is picoliter range and makes analysis time unrealistic (~500 h) for processing clinical sample volumes ($10^2$-$10^3$ nL). Although analyzing a small portion (picoliter range) of the sample is a possible solution, analysis of a diluted sample is difficult due to the limited number of molecules inside the sample ($10^0$ pL × $10^0$ pM = 0.6 molecule). Therefore, a novel ELISA format that has both a nanoliter-volume reaction field and high S/V is desired.

Here we propose a novel format for thin-layered microfluidic ELISA by expanding the concept of nanofluidic ELISA. A millimeter-wide and micrometer-deep thin layer formed by a glass microchannel was utilized as a nanoliter volume and high S/V reaction field for ELISA. To introduce the sample evenly into the high-aspect-ratio (width/depth = $10^3$) channel, a device design which

incorporate a taper-shaped interface between the thin-layered channel and microchannel for sample injection was proposed. In this proof-of-concept study, fluidic control and introduction of the sample were first confirmed using fluorescent molecules. Then, by measuring a standard C-reactive protein (CRP) solution, the working principle of thin-layered ELISA was verified, and the detection performance was evaluated.

## 2. Concept and Principle

### *2.1. Concept behind the thin-layered microfluidic ELISA*

Figure 1 shows a comparison of the reaction fields of bead-based ELISA,[4] thin-layered ELISA, and nanofluidic ELISA.[22] Bead-based ELISA has antibody-immobilized beads (diameter: 40 μm) in a microchannel with a width/depth of $10^2$ μm, enabling rapid and sensitive detection of analyte proteins due to a high S/V reaction field ($10^5$ $m^{-1}$). This format has a reaction field volume of $10^2$ nL, which can be used to process a clinical sample volume ($10^2$-$10^3$ nL) and has been used in on-site blood tests of inflammation[4] and allergy.[5] However, a simpler format without beads is required for further robustness of operation. On the other hand, the nanofluidic format[22] uses an antibody-immobilized nanochannel with a width/depth of $10^2$-$10^3$ nm, enabling single-molecule detection due to an ultra-high S/V ($10^6$ $m^{-1}$) reaction field without beads. However, the volume of the reaction field is $10^0$ pL, and this format cannot be used to process clinical sample volumes.

As shown in Figure 1, we propose a thin-layered ELISA by expanding the concept of nanofluidic ELISA and aiming for a reaction field with a high S/V ($10^5$-$10^6$ $m^{-1}$) and large volume capacity ($10^2$ nL) without beads. From the nanofluidic ELISA format, the channel width and length were expanded $10^3$- and $10^1$-fold, respectively, to increase the volume. The channel depth was maintained as the S/V ratio of the reaction field is determined only by channel depth and is not dependent on channel width (as details in the calculation described in the experimental section).

The high-aspect-ratio (width/depth = $10^3$) of the ELISA reaction field is created on glass due to its

high morphological stability, rigidity, optical transparency, resistance to a wide range of solvents,[23] and availability of high-density surface modification by silane coupling reagents.[24]

*2.2. Conceptual design and working principle*

As shown in Figure 2(a), the thin-layered microfluidic ELISA was designed based on the methodology of micro unit operation (MUO), which was established by our group.[25] The flow of the conceptual design is as follows: (1) A flow chart of chemical process was formulated, (2) The flow chart was divided into unit operations (e.g., antigen-antibody reaction, bound/free separation, etc.), (3) Unit operations were converted into MUOs, which are the unit operations realized in microspace, and (4) Finally, the MUOs are integrated into a microfluidic device.

Figure 2(b) shows an overview of the thin-layered microfluidic ELISA. A thin-layered channel is located on the center of the device, connecting two microchannels for sample injection (transporting channels). A taper-shaped interface was attached to the inlet and the outlet of the thin-layered channel to introduce the sample solution evenly into a high-aspect-ratio channel and to detect most of the reacted substrates collectively by optical detection. Reagents are transported from reagent vials to the thin-layered channel via the transporting channels by external pressure. Using two pressure controllers, the direction of the flow in the thin-layered channel can be controlled, which is important when switching reagents. While replacing the reagent in the transporting channel, the thin-layered channel can be protected from contamination by introducing wash buffer from the other side. Capture antibodies are immobilized on the center of the thin-liquid layer channel (antibody-immobilized region, pink-colored zone in Figure 2(b)), and this antibody-immobilized region functions as the reaction field of ELISA.

The bottom of Figure 2(b) shows the working principle of the thin-liquid ELISA based on the flow chart described in Figure 2(a). The flow of the assay is as follows: (i) For analyte capture by the antigen-antibody reaction, analyte proteins are introduced into the thin-layered channel. While passing through the antibody-immobilized region, the analyte proteins interact with the capture antibodies and

are probabilistically captured. (ii) For bound/free separation, wash buffer is introduced, and the channel is washed thoroughly to remove non-specific binders of analyte proteins or enzyme-labeled antibodies. (iii) For antigen-antibody reaction, enzyme-labeled antibody is introduced into the thin-layered channel, and the sandwich structure of the capture antibody, analyte protein, and enzyme-labeled antibody is formed. (iv) For bound/free separation, wash buffer is introduced again. (v) For the enzymatic reaction, the channel is filled with substrate solution, and the flow is stopped for the enzymatic reaction, allowing accumulation of the colored substrates. (vi) For detection, the flow is re-started, and the colored substrates generated by the enzymatic reaction are detected downstream as a peak by a detector.

The time window of the colored substrates on the antibody-immobilized region (pink zone in Figure 2(b)) to reach the detection point can be calculated from the flow velocity. The peak, whose top is located within the time window, is recognized as a specific signal peak, and the other peaks are considered non-specific peaks. The height of the specific signal peak is taken as the ELISA signal.

## 3. Experimental

### *3.1. Materials*

Borosilicate substrates with thin-layered microfluidic ELISA channels were purchased from the Institute of Microchemical Technologies, Co., Ltd. (Kawasaki, Kanagawa, Japan). (3-aminopropyl) triethoxysilane (APTES) and ethanolamine were purchased from Sigma Aldrich (St. Louis, MO, USA). Bovine serum albumin (BSA) was purchased from Johnson and Johnson (New Brunswick, NJ, USA). CRP and anti-CRP mouse IgG were purchased from Oriental Yeast, Co. Ltd. (Tokyo, Japan) and used as an analyte protein and a capture antibody respectively. Glutaraldehyde was purchased from Fujifilm-Wako Pure Chemical, Co. Ltd. (Tokyo, Japan). Horseradish peroxidase (HRP)-conjugated anti-CRP monoclonal antibody was purchased from Abcam (Cambridge, UK) and used as an enzyme-labeled antibody. Premixed solution of 3,3′,5,5′-tetramethylbenzidine and hydroperoxide solution

were purchased from Seracare Life Sciences, Inc. (Milford, MA, USA) and used as a substrate solution. Silane-polyethylene-glycol (PEG, molecular weight = 5,000) was purchased from Nanocs (New York, NY, USA).

*3.2. Design of thin-layered microfluidic ELISA device*

Figure 3(a) shows the detailed design of the thin-layered channel. As a first step of verification, the S/V ratio of the thin-liquid layer ELISA device was matched with that of the bead-based ELISA to compare the detection performance. The S/V ratio of the thin-layered microfluidic ELISA was calculated according to the equation below:

$$\mathbf{S/V\ ratio} = \frac{\mathbf{The\ area\ of\ the\ functional\ surface}(\boldsymbol{\mu m^2})}{\mathbf{The\ volume\ of\ the\ reaction\ field}(\boldsymbol{\mu m^3})} \#(\mathbf{1})$$

$$= \frac{\boldsymbol{L\,W}}{\boldsymbol{L\,W\,d}} \#(\mathbf{2})$$

$$= \frac{\mathbf{1}}{\boldsymbol{d}} \#(\mathbf{3})$$

where $L$ represents the length of the functional surface, $W$ represents the width of the channel, and $d$ represents the depth of the channel.

In the bead-based format, the S/V ratio was calculated as below:

$$\mathbf{S/V\ ratio} = \frac{\boldsymbol{N\,a}}{\boldsymbol{V}_{\mathbf{channel}}(\mathbf{1}-\boldsymbol{p})} \#(\mathbf{4})$$

where $N$ represents the number of embedded beads, $a$ represents the total area of a bead, $V_{channel}$ represents the volume of the bead-packing part of the microchannel, and $p$ represents the packing factor.

N is calculated as follows:

$$\boldsymbol{N} = \frac{\boldsymbol{V}_{\mathbf{channel}}\,\boldsymbol{p}}{\boldsymbol{V}_{\mathbf{bead}}} \#(\mathbf{5})$$

where $V_{bead}$ represents the volume of a bead. Also, the area and the volume of a bead can be calculated as:

$$\boldsymbol{V}_{\mathbf{bead}} = \frac{\mathbf{4}}{\mathbf{3}}\boldsymbol{\pi r^3} \quad \#(\mathbf{6})$$

$$a = 4\pi r^2 \#(7)$$

where r represents the radius of a bead. Thus, finally, the S/V ratio of the bead-based format is calculated as follows:

$$\text{S/V ratio} = \frac{a\,p}{V_{\text{bead}}(1-p)} \qquad \#(8)$$

$$= \frac{3 \quad p}{r(1-p)} \#(9)$$

From this calculation, the S/V ratio of the bead-based format was 0.19 $\mu m^{-1}$ using a bead radius r = 20 μm and packing factor p = 0.56. Using equation (3), the depth of the channel of thin-layered microfluidic ELISA was determined to be 5.2 μm to match the S/V ratio with that of the bead-based ELISA.

To introduce the sample evenly into the broad thin-liquid layer channel, the taper-shaped channel was attached to the inlet and outlet of the thin-layered channel. The widths of the narrow part and wide part were set to 50 μm and 1000 μm, respectively. The length of the antibody-immobilized region was set to 10 mm to match the bead-based ELISA. The final design of the thin-layered ELISA is shown in Figure 3(a).

*3.3. Fabrication and surface modification*

The borosilicate substrates with the designed channel were purchased from the Institute of Microchemical Technologies, Co., Ltd. For surface modification and bonding of the substrates, the low-temperature bonding method developed by our group[21] was used. Briefly, APTES (Sigma Aldrich) was modified on the cover substrate using vapor phase modification. Subsequently, the modified surface of APTES was partially removed with vacuumed-ultra-violet light. Then, the two substrates were bonded and heated at 110 °C for 3 h. The fabricated device is shown in Figure 3(b).

Antibody was immobilized on the channel surface according to the reported procedure.[21] Briefly, the remaining APTES was first activated by flowing 2.5% glutaraldehyde/borate buffer for 1.5 h. Then, the captured antibody was immobilized by flowing 25 μg/mL anti-CRP mouse IgG (Oriental Yeast)

in phosphate-buffered saline (PBS) for 1 h. Unreacted sites were quenched by ethanolamine by flowing 5 M ethanolamine/PBS for 10 min. To prevent non-specific adsorption of analyte proteins and enzyme-labeled antibodies, the channel was modified with PEG by flowing 1.0 mg/mL silane-PEG (molecular weight = 5,000, Nanocs) for 1.5 h before the immobilization of antibodies. The channel was also coated with BSA by flowing 2.0% BSA/PBS for 30 min just before the experiment. The schematic of the surface treatment of the thin-layered channel is shown at the bottom of Figure 3(a).

*3.4. Experimental setup*

The device was set in the device holder. The two inlet holes of the device were connected to reagent vials, pressure controllers (MFCS-EZ, Fluigent, Paris, France), and an air compressor using capillaries (ICT-55P, Institute of Microchemical Technologies, Tokyo, Japan), connectors (UF-C, Institute of Microchemical Technologies, Tokyo, Japan), and o-rings (AS001, Air Water Mach, Inc., Nagano, Japan), respectively. The liquid inside the channel was controlled by external pressure. For the readout of ELISA, a microscope Eclipse 80i (Nikon Corporation, Japan) equipped with our original detector, a differential interference contrast thermal lens microscope (DIC-TLM)[26] was used. A fluorescence microscope IX-71 (Olympus, Tokyo, Japan) was used for visualization of the flow.

*3.5. Measurement of standard CRP solution with thin-layered microfluidic ELISA*

Standard CRP solution (50 nL of 0.0-3.3 μg/mL) was introduced into the thin-layered channel, and subsequently, the channel was washed with wash buffer (2.0% BSA, 0.05% Tween-20 in PBS). Then, 1.4 μL of 0.1 μg/mL enzyme-labeled antibody solution (dissolved in PBS) was introduced, and subsequently, the channel was washed with wash buffer. After washing, 1.8 μL substrate solution (Sure Blue, Seracare Life Sciences) was introduced, and the flow was stopped for 30 s for enzymatic reaction. Finally, the flow was re-started, and the colored substrates generated by the enzymatic reaction were detected downstream with the DIC-TLM[26] (excitation beam at 660 nm, 20 mW, probe beam at 532 nm, 1.5 mW).

## 4. Results and Discussion

### *4.1. Confirmation of fluidic control in the thin-layered channel*

To investigate the uniform introduction of solutions in the high-aspect-ratio channel of the thin-layered microfluidic ELISA device, the movement of the fluid was visualized with a fluorescent solution. Initially, 1 μM sodium fluorescein/PBS and wash buffer were introduced into the two transporting channels, and the thin-layered channel was filled with wash buffer by applying external pressures of 50 kPa and 70 kPa for the fluorescein solution and wash buffer, respectively. When the external pressure for the wash buffer was turned off, as shown in Figure 4(a), introduction of the fluorescent solution into the thin-layered channel was observed. Figure 4(c) shows the time course of fluorescence images when the fluorescent solution was introduced into the thin-layered channel by applying 50 kPa. A plug-like edge of the fluorescent solution was observed although the sides of the channel were curved due to the longer travel distance in the sides. Thus, uniform introduction of the sample solution into the high-aspect-ratio thin-layered channel via the taper-shaped interface was confirmed.

Then, the controllability of flow velocity in the thin-layered channel was investigated. The average velocity was determined using the arrival-time difference of the fluorescent solution at two different points in the thin-layered channel as shown in Figure 4(a). Figure 4(b) shows the typical time-course monitoring of fluorescence intensity at two different points when 50 kPa is applied. A sharp increase in fluorescence intensity was observed at different time points with different location points. The average velocity was calculated by dividing the distance between the two different points ($L$ [mm]) by the time difference of the onset of the fluorescence increase ($t$ [s]). Figure 4(d) shows the average velocity plotted against the applied external pressure (50, 100, 150 kPa). We confirmed that the average velocity was linearly correlated with the applied pressure. Thus, good controllability of the flow velocity (1.1–3.4 mm/s) in the thin-layered channel by external pressure (50-150 kPa) was confirmed. Based on this result, a sequence of external pressures for ELISA was designed and programmed using

the software (script module of MAESFLO313) for MFCS-EZ (Fluigent).

*4.2. Verification of the working principle by measuring the standard CRP solution*

The working principle of thin-layered microfluidic ELISA was investigated by measuring standard solutions (0.0-3.3 μg/mL) of CRP. The procedure for measurement is as follows. Initially, two transporting channels and a thin-layered channel were filled with wash buffer. For the start of (i) antigen-antibody reaction, the standard solution of CRP was injected into one of the transporting channels by applying 200 kPa for 70 s while the thin-layered channel was protected by the counterflow of wash buffer by applying 250 kPa. Then, 50 nL standard solution was introduced into the thin-layered channel by applying 100 kPa for 6 s. Then, for (ii) bound/free separation, the thin-layered channel was washed by wash buffer at 200 kPa for 20 s. For (iii) antigen-antibody reaction, 0.1 ng/mL HRP-labeled antibody solution was injected into the microchannel by applying pressure (200 kPa) for 70 s, and subsequently the HRP-labeled antibody was introduced into the thin-layered channel at 300 kPa for 40 s. For (iv) bound/free separation, the thin-layered channel was washed with wash buffer at 200 kPa for 20 s. For (v) enzymatic reaction, the substrate solution was injected to the transporting channel by applying 200 kPa for 90 s. Then, the substrate solution was introduced into the thin-layered channel at 340 kPa for 80 s, and the pressure was turned off and the flow was stopped allowing for the enzymatic reaction. After 30 s, for (vi) detection, the substrate solution was introduced again at 340 kPa, while the light absorption at 660 nm due to the colored substrate was monitored downstream with DIC-TLM.[26] The signal was obtained within 6 s after restarting the flow. The timing for each step of the assay was summarized in table 1. The time for each micro unit operation (MUO) can be divided into the time to inject reagent in microchannel (injection time) and the time for operation (operation time). While the operation time is essentially required to realize the assay, the injection time can be reduced by improving the device design. The total assay time was ~7 min for single sample, which is comparable to the beads-based microfluidic ELISA (12 min)[5] and faster than the microfluidic ELISA methods without using beads (~h.).[16]

Figure 5 shows the time course signal of light absorption by DIC-TLM. Specific signal peaks and non-specific signal peaks were distinguished using the time window of the antibody-immobilized region. When the peak top was inside the time window of the antibody-immobilized region, the peak was considered to be a specific signal peak. When the peak top was outside of the time window, the peak was considered to be a non-specific signal peak. As a result, no peaks were observed outside the time window, suggesting that the surface blocking of the nanochannel using PEG (MW = 5,000) and BSA successfully prevented non-specific adsorption of CRP or the HRP-labeled antibody outside the antibody-immobilized region. On the other hand, a non-zero signal was obtained from the blank measurements. This can be attributed to non-specific adsorption of the HRP-labeled antibody to the antibody-immobilized region, where the surface is covered mostly with APTES instead of PEG.

All the specific signal peaks were observed at the location close to the later edge of the time window, and no other peaks were observed within the time window. Considering that the later edge of the time window corresponds to the inlet edge of the antibody-immobilized region, these results suggest that most of the analyte was captured immediately after entering the antibody-immobilized region. This observation supports the possibility that the antibody-immobilized thin-layered channel, which has a high S/V reaction field without beads, can efficiently capture target proteins.

As shown in Figure 5, the heights of specific signal peaks were correlated with the concentration of CRP. Thus, the working principle of thin-layered ELISA was verified. The heights of specific signal peaks were defined as signal values, and as shown in Figure 6(a), a calibration curve was obtained by plotting signals against concentration. The limit of detection (LoD) was 34 ng/mL using the standard deviation of blank measurements (3.3σ). The obtained LoD was lower than the general cut-off values of CRP (1.0 or 3.0 μg/mL), which are the threshold values used for categorize the patients according to the future risk of cardiovascular events; <1.0 μg/mL for low risk, 1.0 - 3.0 μg/mL for intermediate risk, and >3.0 μg/mL for high risk.[27] Thus, the thin-layered ELISA achieved sufficient sensitivity for usage in clinical diagnosis without beads.

To compare the detection performance of thin-layered ELISA with the commercialized bead-based ELISA, a series of standard CRP solutions with different concentration (0.0-4.0 μg/mL) was measured with bead-based ELISA[4,8]. As shown in Figure 6, a calibration curve was obtained by plotting peak heights against concentration, and the LoD was 12 ng/mL. The LoD of thin-layered ELISA (34 ng/mL) was comparable to that of bead-based ELISA (12 ng/mL) using the standard deviation of blank measurements (3.3σ). This result suggests that when the S/V ratio is matched, the thin-layered ELISA can, without beads, detect proteins with similar sensitivity as the commercialized bead-based ELISA. Also, this result supports the concept that the S/V ratio is the determinant of detection sensitivity, and thus, comparable detection performance was achieved without beads.

Based on the concept that detection sensitivity can be controlled by the S/V ratio of the reaction field, thin-layered ELISA has the potential to further improve the detection sensitivity. In thin-layered ELISA, the S/V ratio of the reaction field is inversely proportional to the channel depth as shown in the experimental section. The depth of the current version of the thin-layered channel is 5.2 μm, and an additional decrease is possible, considering that the depth of nanofluidic ELISA[22] is ~800 nm. As almost 100% capture of target proteins and single-molecule-level sensitive detection were confirmed in nanofluidic ELISA, decreasing the depth of thin-layered ELISA will potentially increase the S/V ratio further and enable the detection of even lower concentrations of proteins (e.g., pg/mL), which are difficult to detect by current ELISA systems. To realize an even thinner thin-layered channel, we consider that a device made of glass would be an important factor. The high morphological stability of glass[23] prevents channels from swelling even when the aspect ratio of the channel is high (width/depth >200), and the availability of high-density modification of antibodies (~100 molecules/$\mu m^2$)[21] on a glass surface using silane coupling reagents is expected to contribute to the efficient capture of target proteins.

In medicine, potential needs for ultra-low detection of proteins exist. For example, detection of pg/mL or lower concentrations is required for early detection of cancer, because a large number of

important cancer biomarkers exist at very low levels at early stages of cancer[28]. Moreover, ultra-low detection levels are also important for the immediate detection of relapse after cancer treatment[28]. For such purposes, several potential analytical methods have been developed. For example, liquid chromatography-mass spectrometry (LC/MS) is a high-standard methodology enabling both quantitative and qualitative analysis.[29,30] However, in perspective of time for analysis, it requires time-consuming pre-processing including reduction, alkylation, and digestion of proteins,[31,32] and thus is currently more oriented for basic research of biology. On the other hand, immunoassay can accomplish sensitive and selective detection of the target protein more rapidly than analysis using LC/MS. For example, bulk immunoassay combined with surface enhanced Raman spectrometry (SERS)[33] or surface plasmon resonance (SPR)[34] detection were developed to achieve highly-sensitive detection of CRP at ng/mL However, the long incubation time (~1 h) for antigen antibody reaction is necessary owing to low S/V ratio of the reaction field. To increase the S/V ratio, microfluidic approach is beneficial. Beads-based microfluidic approaches, where the antibody immobilized beads are packed in the microchannel for reaction, have high S/V ratio ($10^2$-fold of a 96-well plate) and can realize sensitive (ng/mL) and rapid (12 min.) detection,[4,5] but it requires complicated fluidic operation. Meanwhile, approaches without using beads, where the capture antibodies are immobilized on the microchannel wall, are free from the complication of fluidics caused by beads, but as the S/V ratio is $10^1$-fold of a 96-well plate and lower than the beads-based approach, long incubation time (~30 min.) is necessary for highly-sensitive detection, leading to the long assay time (~h).[16] Compared to those approaches, the thin-layered ELISA, presented in this study, has high-S/V-ratio reaction field (more than $10^2$-fold of a 96-well plate) and achieved detection of CRP at LOD of 34 ng/mL within 10 min. Furthermore, as mentioned above, the detection sensitivity can be further increased by downsizing the depth of the channel. Though the method requires fluidic control with high pressure (up to 400 kPa) for operation, we believe the thin-layered ELISA can contribute to medicine and biology as a novel platform of sensitive and rapid ELISA. In order to achieve such applications, the optimization of the

assay conditions including S/V ratio of the channel, blocking conditions, concentration of HRP-labeled antibody, velocity of sample introduction and duration of B/F separation are required, and it will be reported in future work.

## 5. Conclusions

To realize sensitive and rapid ELISA without beads, we propose a thin-layered microfluidic ELISA as a novel platform based on our original nanofluidic ELISA. A thin-layer microfluidic channel with millimeter width and micrometer depth was designed to create the reaction field for a large volume ($10^2$ nL) and high S/V ($10^5$-$10^6$ $m^{-1}$), which will lead to large-volume capacity ($10^2$-$10^3$ nL) and high detection sensitivity (ng/mL), respectively. For the proof of concept, a thin-layered microfluidic channel (1.0 mm wide and 5.2 μm deep) with a taper-shaped channel interface was designed and fabricated on borosilicate substrates. Uniform introduction of sample solution into the high-aspect-ratio (200:1) channel was confirmed by visualization of the flow of a fluorescent solution. By measuring a standard CRP solution, the working principle of thin-layered ELISA was verified. The limit of detection (34 ng/mL) was comparable to that of the commercialized bead-based ELISA (12 ng/mL), whose reaction field has the same S/V ratio. Thin-layered ELISA has the potential to further improve the detection sensitivity by further increasing the S/V ratio with lower depth. We believe that thin-layered ELISA can contribute to medicine and biology as a novel platform of sensitive and rapid ELISA.

## Conflicts of interest

There are no conflicts to declare.

## Acknowledgements

The authors gratefully acknowledge financial support from the CREST (Core Research for

Evolutional Science and Technology) JPMJCR14G1 and Grant-in-Aid for JSPS Fellows 17J10031.

## References


1 A. Perrier, J. Gligorov, G. Lefèvre and M. Boissan, *Lab. Investig.*, 2018, **98**, 696–707.

2 W. J. Catalona and S. Loeb, 2010, **8**, 1–9.

3 D. Wild and E. Kodak, *The Immunoassay Handbook*, 2013.

4 K. Sato, M. Tokeshi, T. Odake, H. Kimura, T. Ooi, M. Nakao and T. Kitamori, *Anal. Chem.*, 2000, **72**, 1144–1147.

5 T. Ohashi, K. Mawatari, K. Sato, M. Tokeshi and T. Kitamori, *Lab Chip*, 2009, **9**, 991.

6 K. Sato, M. Yamanaka, H. Takahashi, M. Tokeshi, H. Kimura and T. Kitamori, *Electrophoresis*, 2002, **23**, 734–739.

7 K. Sato, M. Tokeshi, H. Kimura and T. Kitamori, *Anal. Chem.*, 2001, **73**, 1213–1218.

8 E. Mori, T. Oohashi, H. Imai, K. Mawatari and T. Kitamori, *Anal. Methods*, 2017, **9**, 2830–2834.

9 M. Herrmann, E. Roy, T. Veres and M. Tabrizian, *Lab Chip*, 2007, **7**, 1546–1552.

10 J. Park, V. Sunkara, T. H. Kim, H. Hwang and Y. K. Cho, *Anal. Chem.*, 2012, **84**, 2133–2140.

11 E. K. Sackmann, A. L. Fulton and D. J. Beebe, *Nature*, 2014, **507**, 181–189.

12 S. I. Funano, T. G. Henares, M. Kurata, K. Sueyoshi, T. Endo and H. Hisamoto, *Anal. Biochem.*, 2013, **440**, 137–141.

13 X. Tan, M. K. Khaing Oo, Y. Gong, Y. Li, H. Zhu and X. Fan, *Analyst*, 2017, **142**, 2378–2385.

14 K. Eyer, S. Stratz, P. Kuhn, S. K. Küster and P. S. Dittrich, *Anal. Chem.*, 2013, **85**, 3280–3287.

15 Q. Shi, L. Qin, W. Wei, F. Geng, R. Fan, Y. Shik Shin, D. Guo, L. Hood, P. S. Mischel and J. R. Heath, *Proc. Natl. Acad. Sci.*, 2012, **109**, 419–424.

16 Y. Xianyu, J. Wu, Y. Chen, W. Zheng, M. Xie and X. Jiang, *Angew. Chemie - Int. Ed.*, 2018, **57**, 7503–7507.

17 W. C. Sung, H. H. Chen, H. Makamba and S. H. Chen, *Anal. Chem.*, 2009, **81**, 7967–7973.

18 M. Ikami, A. Kawakami, M. Kakuta, Y. Okamoto, N. Kaji, M. Tokeshi and Y. Baba, *Lab Chip*, 2010, **10**, 3335–3340.

19 A. Hibara, T. Saito, H. B. Kim, M. Tokeshi, T. Ooi, M. Nakao and T. Kitamori, *Anal. Chem.*, 2002, **74**, 6170–6176.

20 T. Tsukahara, K. Mawatari, A. Hibara and T. Kitamori, *Anal. Bioanal. Chem.*, 2008, **391**, 2745–2752.

21 K. Shirai, K. Mawatari and T. Kitamori, *Small*, 2014, **10**, 1514–1522.

22 K. Shirai, K. Mawatari, R. Ohta, H. Shimizu and T. Kitamori, *Analyst*, 2018, **143**, 943–948.

23 K. Ren, J. Zhou and H. Wu, *Acc. Chem. Res.*, 2013, **46**, 2396–2406.

24 L. T. Zhuravlev and V. V. Potapov, *Russ. J. Phys. Chem.*, 2006, **80**, 1119–1128.

25 M. Tokeshi, T. Minagawa, K. Uchiyama, A. Hibara, K. Sato, H. Hisamoto and T. Kitamori, *Anal. Chem.*, 2002, **74**, 1565–1571.

26 H. Shimizu, K. Mawatari and T. Kitamori, *Anal. Chem.*, 2009, **81**, 9802–9806.

27 J. Pereira, A. Ribeiro, J. Ferreira-Coimbra, I. Barroso, J. T. Guimarães, P. Bettencourt and P. Lourenço, *BMC Cardiovasc. Disord.*, 2018, **18**, 1–8.

28 J. F. Rusling, C. V. Kumar, J. S. Gutkind and V. Patel, *Analyst*, 2010, **135**, 2496–2511.

29 A. Scherl, *Methods*, 2015, **81**, 3–14.

30 S. K. G. Grebe and R. J. Singh, *TrAC - Trends Anal. Chem.*, 2016, **84**, 131–143.

31 D. Keith Williams and D. C. Muddiman, *J. Proteome Res.*, 2009, **8**, 1085–1090.

32 O. P. Bondar, D. R. Barnidge, E. W. Klee, B. J. Davis and G. G. Klee, *Clin. Chem.*, 2007, **53**, 673–678.

33 F. M. Campbell, A. Ingram, P. Monaghan, J. Cooper, N. Sattar, P. D. Eckersall and D.

Graham, *Analyst*, 2008, **133**, 1355–1357.

34 W. Wang, Z. Mai, Y. Chen, J. Wang, L. Li, Q. Su, X. Li and X. Hong, *Sci. Rep.*, 2017, **7**, 1–8.

**Figure captions**

**Figure 1.** Concept of thin-layered microfluidic ELISA.

**Figure 2.** (a) Conceptual design and (b) working principle of the thin-layered microfluidic ELISA device. Ag, Ab, and B/F represent antigen, antibody, and bound/free, respectively.

**Figure 3.** Detailed design and fabricated thin-layered microfluidic ELISA device. (a) Detailed design and surface coating of the thin-layered channel. (b) Photographic images of the fabricated device.

**Figure 4.** Confirmation of fluidic control by visualization of the flow of a fluorescent solution. (a) Schematic diagram showing monitoring of the fluorescence intensity. (b) Time course of fluorescence intensity at positions A and B. The time difference of the onset of the fluorescence increase was used to calculate the velocity. (c) Typical time course of fluorescence images when 50 kPa is applied. (d) Average velocity plotted against the applied pressure.

**Figure 5.** Obtained ELISA signal from measurement of a standard CRP solution. The concentrations of CRP are at (a) 0.0 μg/mL, (b) 0.4 μg/mL (c) 1.0 μg/mL and (d) 3.3 μg/mL.

**Figure 6.** Comparison of the calibration curve of CRP measurement by (a) thin-layered microfluidic ELISA and (b) Beads-based microfluidic ELISA. Error bars represent $2\sigma$ (N = 3).

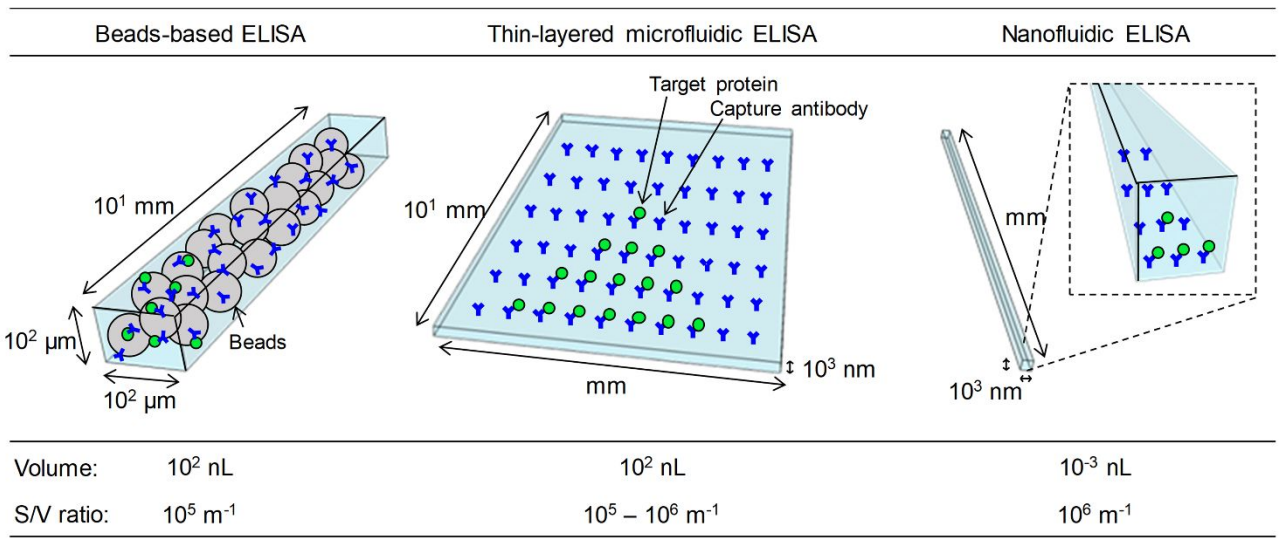
Beads-based ELISA
Thin-layered microfluidic ELISA
Nanofluidic ELISA
$10^1$ mm
$10^2$ µm
$10^2$ µm
Beads
Target protein
Capture antibody
$10^1$ mm
mm
$10^3$ nm
mm
$10^3$ nm
Volume: $10^2$ nL $10^2$ nL $10^{-3}$ nL
S/V ratio: $10^5$ m$^{-1}$ $10^5 – 10^6$ m$^{-1}$ $10^6$ m$^{-1}$

Figure 1.

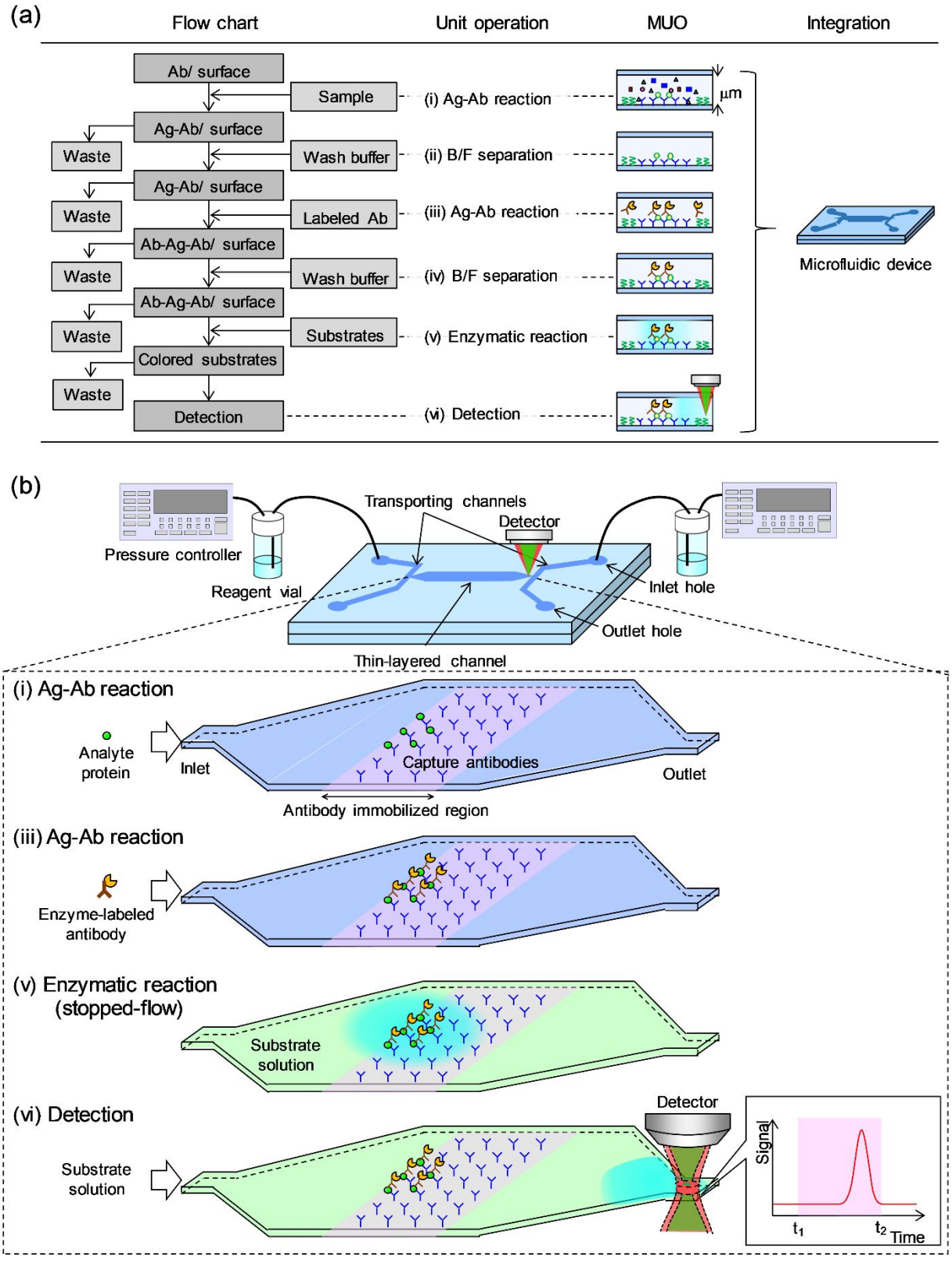
(a)
Flow chart
Unit operation
MUO
Integration
Ab/ surface
Sample
(i) Ag-Ab reaction
μm
Ag-Ab/ surface
Waste
Wash buffer
(ii) B/F separation
Ag-Ab/ surface
Waste
Labeled Ab
(iii) Ag-Ab reaction
Ab-Ag-Ab/ surface
Waste
Wash buffer
(iv) B/F separation
Ab-Ag-Ab/ surface
Waste
Substrates
(v) Enzymatic reaction
Colored substrates
Waste
Detection
(vi) Detection
Microfluidic device
(b)
Pressure controller
Transporting channels
Detector
Reagent vial
Inlet hole
Outlet hole
Thin-layered channel
(i) Ag-Ab reaction
Analyte protein
Inlet
Capture antibodies
Outlet
Antibody immobilized region
(iii) Ag-Ab reaction
Enzyme-labeled antibody
(v) Enzymatic reaction (stopped-flow)
Substrate solution
(vi) Detection
Substrate solution
Detector
Signal
t1
t2
Time

Figure 2.

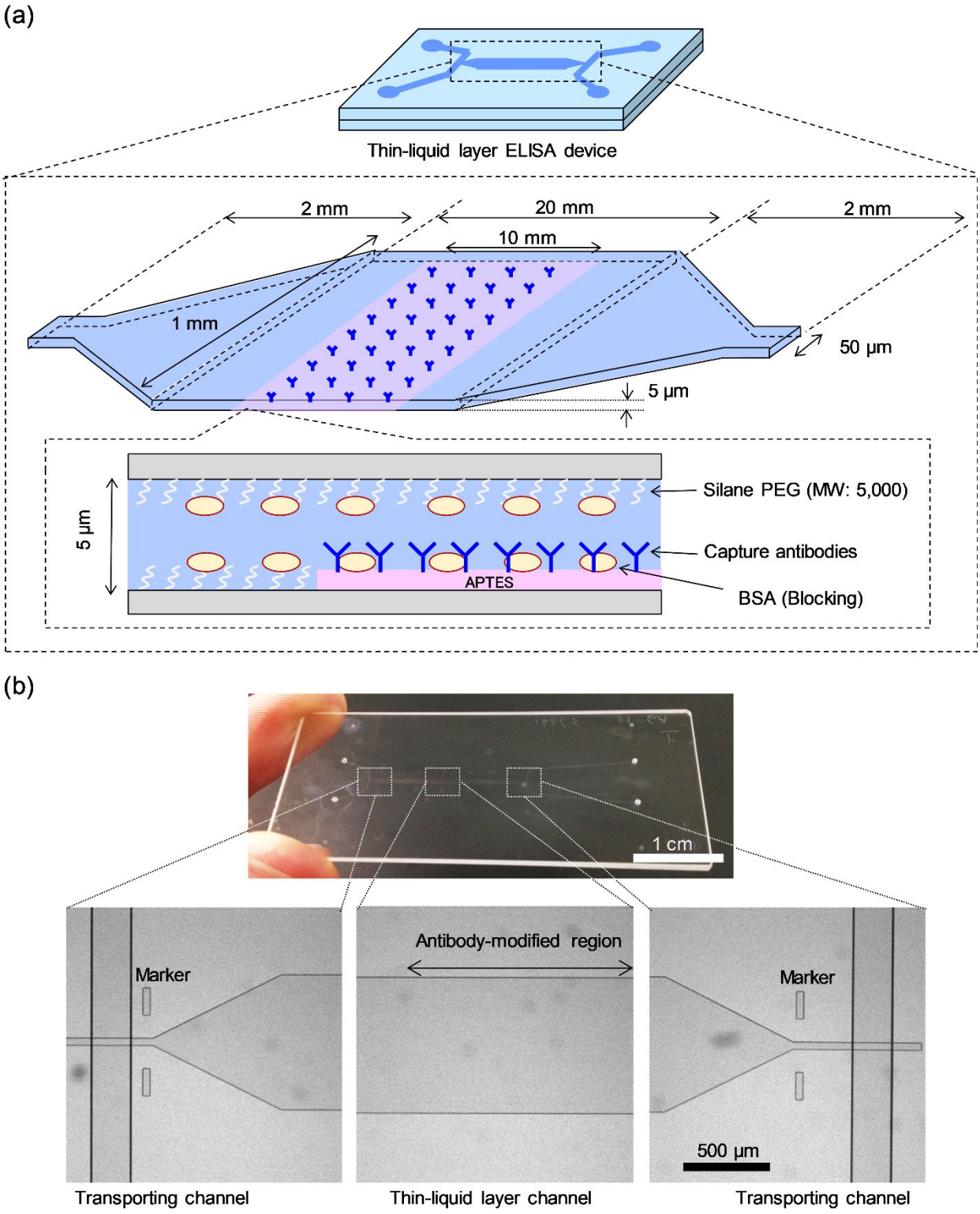
(a)
Thin-liquid layer ELISA device
2 mm
20 mm
2 mm
10 mm
1 mm
50 μm
5 μm
5 μm
Silane PEG (MW: 5,000)
Capture antibodies
APTES
BSA (Blocking)
(b)
1 cm
Marker
Antibody-modified region
Marker
500 μm
Transporting channel
Thin-liquid layer channel
Transporting channel

Figure 3.

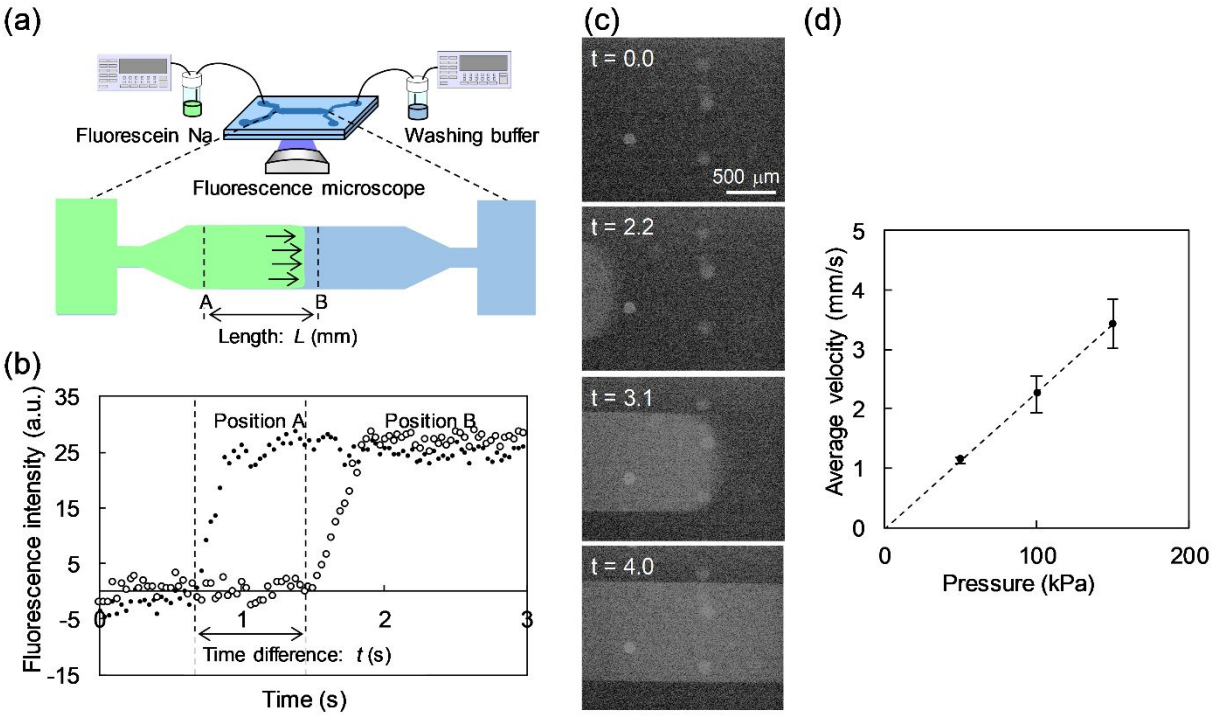
(a)
Fluorescein Na
Washing buffer
Fluorescence microscope
A
B
Length: L (mm)
(b)
Fluorescence intensity (a.u.)
Position A
Position B
Time difference: t (s)
Time (s)
(c)
t = 0.0
500 μm
t = 2.2
t = 3.1
t = 4.0
(d)
Average velocity (mm/s)
Pressure (kPa)

Figure 4.

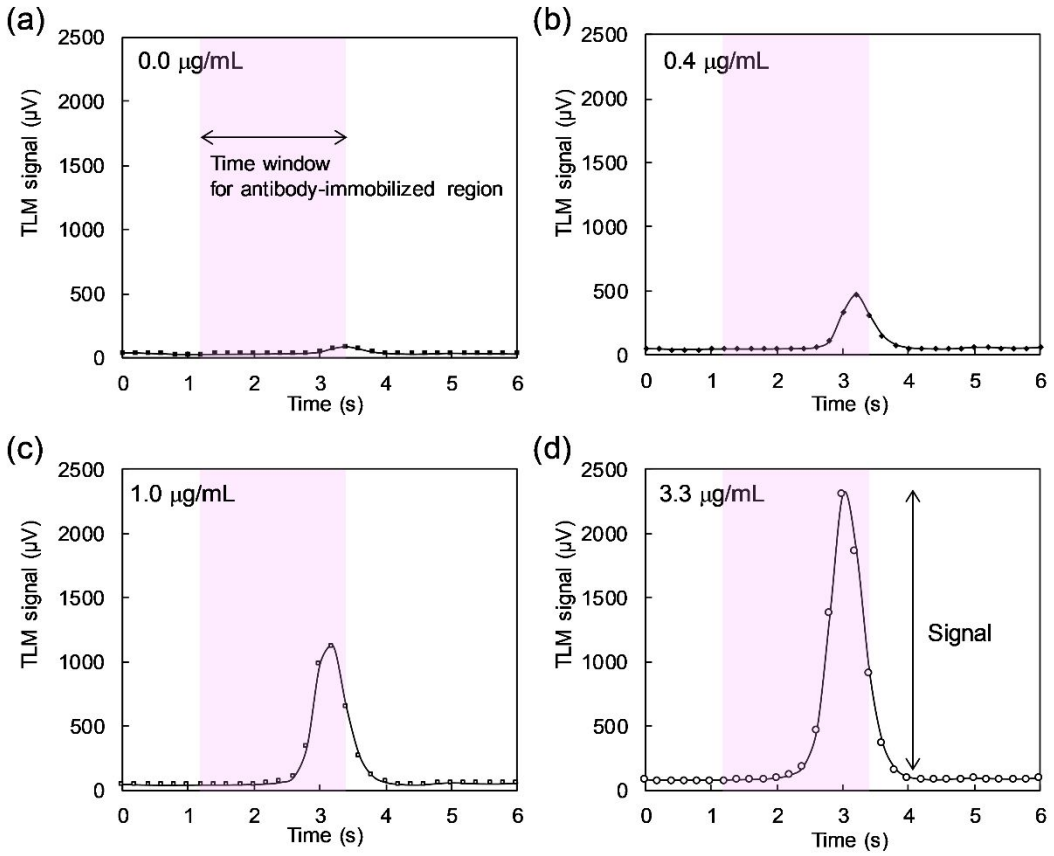
(a)
0.0 μg/mL
Time window
for antibody-immobilized region
TLM signal (μV)
Time (s)
(b)
0.4 μg/mL
TLM signal (μV)
Time (s)
(c)
1.0 μg/mL
TLM signal (μV)
Time (s)
(d)
3.3 μg/mL
Signal
TLM signal (μV)
Time (s)

Figure 5.

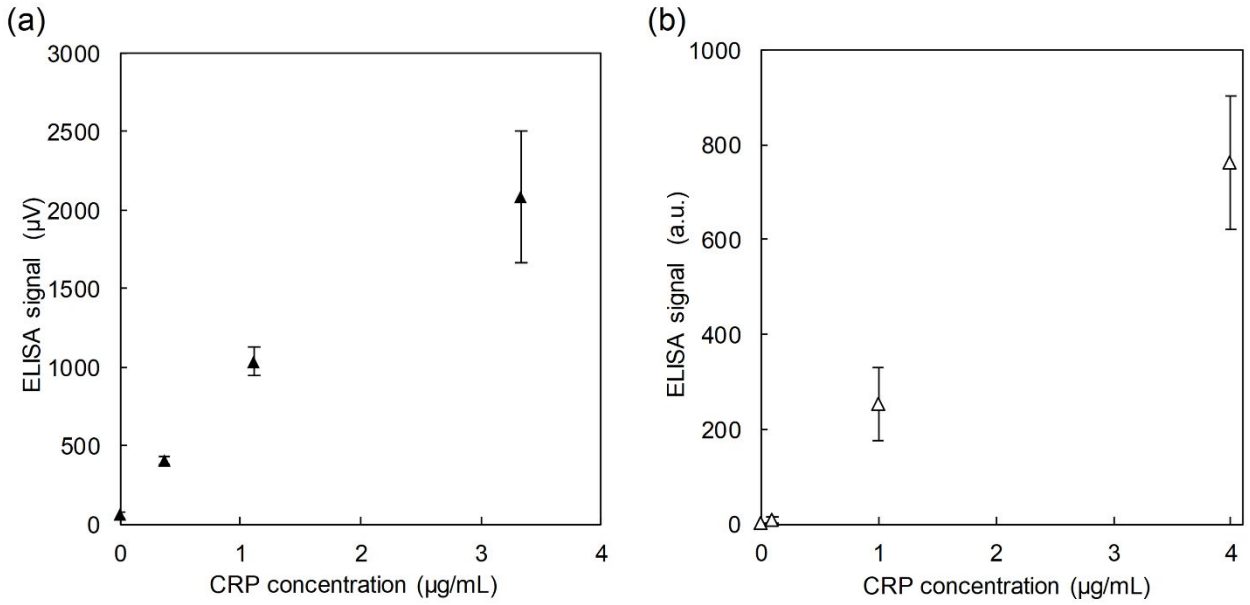
(a)
3000
2500
2000
1500
1000
500
0
ELISA signal (μV)
0
1
2
3
4
CRP concentration (μg/mL)
(b)
1000
800
600
400
200
0
ELISA signal (a.u.)
0
1
2
3
4
CRP concentration (μg/mL)

Figure 6.

Table 1. Timing for each step of the assay by 6 MUOs. The time for each MUO is divided into the time to inject reagent in microchannel (injection time) and the time for operation (operation time)

| No. | MUO | Injection time (s) | Operation time (s) | Total (s) |
|---|---|---|---|---|
| (i) | Ag-Ab reaction | 70 | 6 | 76 |
| (ii) | B/F separation | 0 | 20 | 20 |
| (iii) | Ag-Ab reaction | 70 | 41 | 111 |
| (iv) | B/F separation | 0 | 20 | 20 |
| (v) | Enzymatic reaction | 170 | 30 | 200 |
| (vi) | Detection | 0 | 6 | 6 |
| | Total | 310 | 123 | 433 |

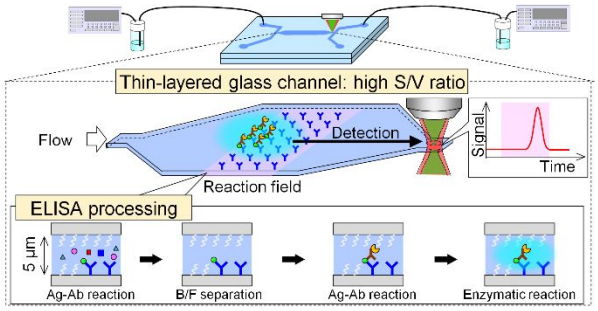


Graphical abstract

An antibody-immobilized thin-layered glass microfluidic channel with the high surface-to-volume ratio was developed for rapid and sensitive enzyme-linked immunosorbent assay.

(20 words)